Signal Recognition Particle *Alu* Domain Occupies a Defined Site at the Ribosomal Subunit Interface upon Signal Sequence Recognition†

Lionel Terzi,‡ Martin R. Pool,§,|| Bernhard Dobberstein,§ and Katharina Strub*,‡

Université de Genève, Département de Biologie Cellulaire, CH-1211 Genève 4, Switzerland, and Zentrum für Molekularbiologie, Heidelberg, Im Neuenheimer Feld 282, 69120 Heidelberg, Germany

Received August 4, 2003; Revised Manuscript Received October 3, 2003

ABSTRACT: The eukaryotic signal recognition particle (SRP) is essential for cotranslational targeting of proteins to the endoplasmic reticulum (ER). The SRP *Alu* domain is specifically required for delaying nascent chain elongation upon signal sequence recognition by SRP and was therefore proposed to interact directly with ribosomes. Using protein cross-linking, we provide experimental evidence that the *Alu* binding protein SRP14 is in close physical proximity of several ribosomal proteins in functional complexes. Cross-linking occurs even in the absence of a signal sequence in the nascent chain demonstrating that SRP can bind to all translating ribosomes and that close contacts between the *Alu* domain and the ribosome are independent of elongation arrest activity. Without a signal sequence, SRP14 cross-links predominantly to a protein of the large subunit. Upon signal sequence recognition, certain cross-linked products become detectable or more abundant revealing a change in the *Alu* domain−ribosome interface. At this stage, the *Alu* domain of SRP is located at the ribosomal subunit interface since SRP14 can be cross-linked to proteins from the large and small ribosomal subunits. Hence, these studies reveal differential modes of SRP−ribosome interactions mediated by the *Alu* domain.

Ribosomes translating mRNAs coding for secretory and membrane proteins are specifically targeted to the endoplasmic reticulum (ER) membrane by a cytosolic ribonucleoprotein particle, the signal recognition particle (SRP) (for review, see ref *1*). The specificity of this process is ensured by the presence of a signal sequence in the growing peptide chain, which is recognized by SRP when it emerges from the ribosome. Signal sequence recognition by SRP causes a slow down or an arrest in the elongation of the nascent chain (*2*, *3*). The SRP−ribosome−nascent chain complex is then targeted to the ER via the interaction of SRP with its membrane receptor, the SRP receptor (SR), a heterodimeric membrane protein (*4*, *5*). SR coordinates the release of SRP from the ribosome with the insertion of the nascent chain into the Sec61 complex, the aqueous translocation pore in the ER membrane (for reviews, see refs *6* and *7*). Free SRP can then engage in another targeting round, and membrane-associated ribosomes resume translation at their regular speed, leading to the cotranslational transfer of the nascent chain across or into the ER membrane. As emphasized by this model, SRP is proposed to play a critical role in the precise accommodation of the translational machinery to the translocation process. From this point of view, it appears that the ability of SRP to interact with and to modulate the activity of the translating ribosome is a major requirement for its function.

Mammalian SRP is composed of a small RNA, SRP RNA, and six polypeptides named according to their apparent molecular mass (SRP9, 14, 19, 54, 68, and 72). SRP54 recognizes the signal sequence and mediates targeting to the ER membrane by binding to SR in a GTP-controlled manner (*8*, *9*). SRP9/14 and the 5′ and 3′ ends of SRP RNA form the *Alu* domain of SRP, which mediates elongation arrest activity. Elongation arrest is detected in vitro as a complete arrest or a transient delay in the elongation of the nascent chain, and its absence decreases the translocation efficiency (*10*−*12*). In vivo, it is required for the tight accommodation of the translation and the translocation processes (*13*). Removal of the *Alu* domain or the protein SRP9/14 abrogates the elongation arrest activity of the particle (*10*, *14*).

Many SRP activities appear to depend on interactions with the ribosome. The ribosome may play an important role in signal sequence recognition by SRP54 since SRP fails to bind signal sequences of nascent chains that have been released from the ribosome (*15*, *16*). In addition, a ribosomal component stimulates GTP binding of SRP54 for an interaction with SR (*17*). Recently, two ribosomal proteins in proximity to the nascent chain exit site have been shown to interact in two distinct modes with SRP54 before and after binding to SR (*18*). Together with the finding that the yeast homologues of the two ribosomal proteins form major contacts with the translocon complex Sec61p (*19*), these

† This work was supported by grants from the Swiss National Science Foundation, the Canton of Geneva, and the MEDIC Foundation. B.D. and K.S. wish to acknowledge long-term support from the European Union Framework IV TMR program for SRPNET (FMRX-CT960035) and Framework V Quality of Life program for MEMPROT-NET (QLK3-CT200082). M.R.P. was a fellow of the TMR program SRPNET.

* To whom correspondence should be addressed. Telephone: +41-22-379 6724. Fax: +41-22-379 3221. E-mail: strub@cellbio.unige.ch.

‡ Université de Genève.

§ Zentrum für Molekularbiologie.

|| Current address: University of Manchester, School of Biological Sciences, 2.205 Stopford Building, Oxford Road, Manchester, M13 9PT, UK.

10.1021/bi0353777 CCC: $27.50
Published on Web 12/09/2003

studies suggested that SR-regulated contacts of SRP54 with the ribosome may control ribosome binding to the translocon. Bacterial SRP can also be cross-linked to the same ribosomal protein as well as to ribosomal RNA near the nascent chain exit site (*20*, *21*). On the basis of the observation that SRP affects nascent chain elongation, it was proposed that the *Alu* domain of SRP might bind in the ribosomal A-site (*22*, *23*), possibly by mimicking tRNA. However, structural studies failed to reveal a significant structural mimicry between the *Alu* domain and tRNA (*24*). A mutational analysis of SRP14 revealed that a short C-terminal region is very critical for elongation arrest activity (*12*, *13*), indicating that direct contacts between the *Alu* domain, and possibly more specifically, between SRP14 and the ribosome may be essential for the delay in nascent chain elongation. However, physical proximity and/or a direct contact between the *Alu* domain and the ribosome have so far not been experimentally documented, and the mechanism of the elongation arrest function remains to be elucidated.

Here, we probe the molecular environment of SRP14 in functional SRP−ribosome complexes of mammalian and plant translation systems using a bifunctional cross-linker. In both systems, SRP14 is in close proximity to several ribosomal proteins. In addition, the four cross-linked products have comparable sizes defining a conserved *Alu* domain-binding site in the ribosome. With ribosomes bearing nascent chains lacking a signal sequence and vacant ribosomes, SRP14 cross-links predominantly to a protein of the large ribosomal subunit. Upon signal sequence recognition, three other cross-linked products become more abundant, revealing a change in the *Alu* domain−ribosome interface. SRP14 is now cross-linked to ribosomal proteins of the large and small subunits in agreement with its location at the subunit interface of the ribosome. Taking into account the complexity and the apparent minimal sizes of the cross-linked products as well as the location of the *Alu* domain at the ribosomal subunit interface, we present a schematic model for the SRP *Alu* domain-binding site.

MATERIAL AND METHODS

In Vitro Transcriptions. Cyc130 and pPl86 mRNAs, encoding the first 130 and 86 amino acids of cyclin and preprolactin, respectively, were synthesized with SP6 RNA polymerase (Promega) from plasmids pCyclin and pSP-BP4 (*12*, *25*) linearized with *Pst*I and *Pvu*II, respectively. Full-length cyclin and preprolactin mRNAs were produced from the same plasmids linearized with *Eco*RI.

Purification of Ribosome-Nascent Chain Complexes. RNCs were produced in 100 μL translations with nuclease-treated rabbit reticulocyte lysate (Promega) programmed individually with optimized amounts of truncated Cyc130 and pPl86 mRNAs (see below) in the presence of 40 μM cold methionine. No mRNA was added to the mock translations. After translation for 30 min at 30 °C, synthesis was stopped with cycloheximide (final concentration, 0.5 mM), and the salt concentrations of the samples were adjusted to 500 mM potassium acetate (KOAc) and 5 mM magnesium acetate ($Mg(OAc)_2$) in a final volume of 200 μL. After 15 min on ice, reactions were centrifuged 5 min at 15 000 rpm to pellet aggregates. Aliquots of 100 μL of the supernatants were loaded on 2 mL sucrose cushions (20 mM HEPES pH 7.5, 500 mM KOAc pH 7.5, 5 mM $Mg(OAc)_2$ pH 7.5, 500 mM sucrose, 2 mM DTT, 0.01% Nikkol, 0.5 mM cycloheximide) and centrifuged in a TFT80.4 rotor (Kontron) for 1 h at 50 000 rpm at 4 °C. Ribosomal pellets were resuspended in 20 μL of $HKMND^{50-2.5-1}$ (20 mM HEPES pH 7.5, 50 mM KOAc pH 7.5, 2.5 mM $Mg(OAc)_2$ pH 7.5, 0.01% Nikkol, 1 mM DTT). The concentrations of ribosomes were determined as described (*26*). RNC yields were optimized by titrating the synthetic mRNAs into translation reactions containing [^{35}S]-methionine (>37 Tbq/mmol, Amersham Pharmacia Biotech). Ribosomal pellets were obtained as stated previously and analyzed by 5−20% SDS−PAGE and autoradiography. Cyc130 and pPl86 nascent chains were quantified with a phosphorescence imaging system (BioRad), and their relative yields were calculated taking into account that the pPl86 and Cyc130 nascent chains contain four and six methionines residues, respectively. Maximal yields of Cyc130 and pPl86 were obtained with a 6- and 16-fold excess of mRNA over ribosomes, respectively. RNCs were also produced in 100 μL translations with wheat germ extract at 26 °C and purified as described previously. However, under optimized translation conditions, the yields of RNC formation were always lower with the wheat germ lysate (about 5-fold) when compared to the rabbit reticulocyte lysate (results not shown). SRP could therefore not be saturated with pPl86 ribosomes as described for rabbit SRP-RNC cross-linking (see Results).

Antibody Purification and Immunoblotting. Anti-SRP14 antibodies were purified as described previously (*27*). Anti-L9 and anti-S15 antibodies were raised in rabbits against the peptides CKNKDIRKFLDGIY and KKKRTFRKFTY-RGC, respectively (Sigma-Genosys). For immunoblotting, proteins were separated by SDS−PAGE and transferred on nitrocellulose membranes (Protran BA83). Membranes were blocked 1 h at room temperature with TBS containing 0.2% Tween 20 and 5% nonfat, dry milk (TBST + milk). Incubation with primary antibodies was performed overnight at 4 °C in TBST + milk. Washes were performed in TBST. Membranes were incubated at room temperature with goat anti-rabbit HRP-conjugated antibodies (BioRad) in TBST + milk for 1 h. After washes with TBST, membranes were incubated in Supersignal (Pierce). Images were taken with a CCD camera-based system (GeneGnome, Syngene) and quantified with GeneTools (Syngene). If the membrane had to be tested with several antibodies, it was washed with 5 M urea, 10 mM dithiothreitol (DTT) for several hours at 37 °C, blocked in TBST + milk, and reused as before.

Cross-Linking Assays with Purified RNCs. SRP-RNC complexes were formed individually by incubating 2 pmol of ribosomes, pPl86 RNCs, or Cyc130 RNCs with 1 pmol of canine SRP purified as described before (*28*) in a final volume of 30 μL of $HKMND^{50-2.5-1}$ at 26 °C for 10 min. Prior to incubating with DSS (suberic acid (bis *N*-hydroxy-succinimide ester) supplied from Sigma, 40 mM fresh stock solution in DMSO diluted to a final concentration of 800 μM) at 26 °C for 30 min, the volume was increased to 100 μL with $HKMND^{50-2.5-1}$. The reactions were quenched with 100 mM Tris pH 7.5 for 15 min on ice, TCA-precipitated (10%), and analyzed by 12% SDS−PAGE and by immunoblotting with anti-SRP14 antibodies. Signals for 14-X45, 14-X31, and 14-X20 were quantified. The intensity of each cross-linked product in the reaction with Cyc130 RNCs was

arbitrarily set to 100% and used as a standard to calculate the relative intensity of the equivalent cross-linked product in reactions with ribosomes and pPl86 RNCs. To be able to compare the 14-X45 and 14-X31 signals between different reactions, we first had to normalize the intensities of all cross-linked products in the pPl86 and in the ribosomes reactions to equal intensities of 14-X20 in all reactions. This resulted in only minor adjustments because the 14-X20 intensities were nearly equal in all reactions. Cross-linking reactions under high salt conditions were performed and analyzed as described previously, but prior to incubating with DSS, cycloheximide (final concentration, 0.5 mM) was added to all reactions, and salt concentrations were increased to 500 mM KOAc and 5 mM $Mg(OAc)_2$ where indicated.

Cross-Linking Assay in Ongoing Translations. Rabbit reticulocyte translation reactions (25 μL, 150 mM KOAc, and 2 mM $Mg(OAc)_2$) primed individually with full-length cyclin and preprolactin synthetic mRNAs were incubated at 30 °C for 15 min in the presence or absence of 4 pmol of exogenous canine SRP. The amount of mRNAs in the reactions was chosen to obtain the same translational efficiency of cyclin and preprolactin (see below). Mock translations contained no synthetic mRNA. Prior to incubation with DSS (800 μM final) at 30 °C for 30 min, the volume was increased to 100 μL with $HKMND^{150-2-1}$. The reactions were quenched with 100 mM Tris pH 7.5 for 15 min on ice. Cycloheximide (final concentration, 0.5 mM) was added, and the salt concentration of the samples was adjusted to 500 mM KOAc and 5 mM $Mg(OAc)_2$ in a final volume of 150 μL. After 15 min on ice, reactions were centrifuged 5 min at 15 000 rpm to pellet aggregates. The supernatants were loaded on 2 mL sucrose cushions, and ribosomes were pelleted as stated previously. The ribosomal pellets were directly analyzed by 12% SDS−PAGE and by immunoblotting with anti-SRP14 and anti-S15 antibodies. Translational efficiencies of cyclin and preprolactin were compared by titrating the synthetic mRNAs into translation reactions containing [^{35}S]-methionine in the absence of exogenous canine SRP. Aliquots of 5 μL of the reactions were directly analyzed by 15% SDS−PAGE and autoradiography. Cyclin and preprolactin were quantified with a phosphorescence imaging system (BioRad), and their relative yield was calculated by taking into account that the preprolactin and cyclin chains contain eight and 16 methionines residues, respectively. Similar efficiencies of cyclin and preprolactin synthesis were obtained with 2.5 and 6.8 μg of mRNA, respectively.

Ribosomal Subunit Separation. Complexes were formed with 21 pmol of pPl86 RNC and 17.5 pmol of canine SRP and incubated for 10 min at 26 °C in a final volume of 100 μL (final salt concentration, 60 and 2.5 mM KOAc and $Mg(OAc)_2$, respectively). Cross-linking was done as before but with 100 μM DSS. To separate the ribosomal subunits, reactions were adjusted to 500 mM KOAc, 10 mM $Mg(OAc)_2$, 1 mM puromycin, and 1 mM GTP in a final volume of 150 μL and incubated for 30 min at 37 °C. Ribosomal subunits were separated by centrifugation through 11.2 mL, 10−30% sucrose gradients ($HKMND^{500-10-2}$) for 5.30 h in a TST41.14 rotor (Kontron) at 4 °C and 41 000 rpm. Fractions of 200 μL were collected using Auto Densi-FlowII C (Buchler Instruments), and the absorbance was monitored at 254 nm with an Econo UV-Monitor EM-1 (BioRad). On the basis of the A_{254} profile, the fractions were pooled to represent the 40S and 60S subunits, as well as the 80S ribosomes (see below). Fractions of the top of the gradient were arbitrarily split in four groups. Pooled fractions were TCA-precipitated and analyzed by 12% SDS−PAGE and immunoblotting with anti-SRP14, anti-L9, and anti-S15 antibodies. The L9 and S15 signals confirmed the correct assignments of the fractions. The signals of L9, S15, and the cross-linked products 14-X45, 14-X31, and 14-X20 were quantified for each fraction. All measured signals for the same protein were summed, and for comparison, the signal in each fraction was expressed as a percentage of this sum. Cyc130 RNC-SRP complexes were analyzed the same way, but only S15, L9, and 14-X20 were quantified. To clearly identify the subunit fractions on the basis of the A_{254} profile, Cyc130 RNCs were reacted with DSS (100 μM), and the ribosomal subunits were separated as stated previously. Twenty fractions were collected with continuous monitoring of the absorbance at 254 nm. Fractions were TCA-precipitated and analyzed by 12% SDS−PAGE and immunoblotting with anti-L9 and anti-S15 antibodies. The signals of L9 and S15 were quantified for each fraction. All measured signals for the same protein were summed, and for comparison, the signal in each fraction was expressed as a percentage of this sum. L9 and S15 distribution confirmed the identification of the 40S and 60S subunit, as well as 80S cross-linked ribosomes, using the A_{254} profile. The INT fraction contained both 40S and 60S subunits.

Data Collection of Ribosomal Proteins. Swiss-Prot Protein Knowledgebase for ribosomal proteins: http://igweb.integratedgenomics.com/Bioinformatics/Nikos/Ribosome/rproteins.html contains lists of ribosomal protein families (@SWISS-PROT by Amos Bairoch).

RESULTS

The Alu Domain Has Conserved Binding Sites on the Ribosome. To examine the molecular environment of SRP14 in SRP bound to mammalian and plant ribosome-nascent chain complexes (RNC), we used the homobifunctional cross-linker DSS (Materials and Methods). DSS makes covalent noncleavable bonds to neighboring proteins through amino groups of lysyl side chains spanning a distance of at most 12 Å. The results of the cross-linking experiments were analyzed by SDS−PAGE followed by immunoblotting with affinity-purified anti-SRP14 antibodies (Materials and Methods).

RNCs were formed in reticulocyte lysate using truncated mRNAs encoding the N-terminal 86 and 130 amino acid residues of preprolactin (pPl86) and cyclin (Cyc130), respectively. RNCs were then purified by centrifugation through a sucrose cushion at 500 mM salt to remove translation factors, other cytoplasmic components, and in the absence of a signal sequence in the nascent chain, also endogenous SRP. Rabbit SRP has previously been shown to be present and active in reticulocyte lysate (*5*, *11*). After purification, both nascent chains were detected as single bands of the sizes expected for the truncated proteins (Figure 1A). The absence of shorter translation products demonstrated that each translated mRNA molecule was associated with only one ribosome. To minimize the amount of vacant ribosomes in the RNC preparations (*29*), we saturated pPl86

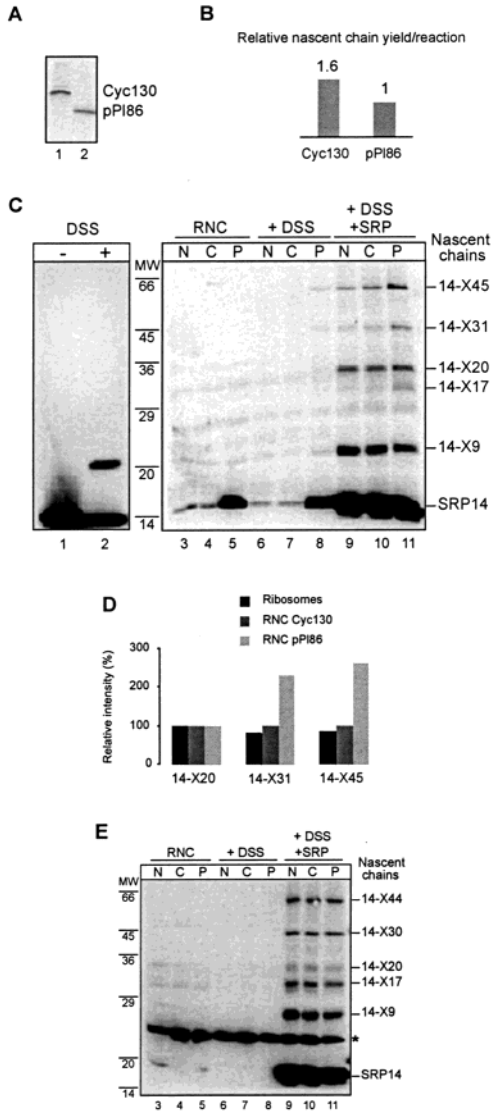

FIGURE 1: Cross-linking of the *Alu* domain-binding protein SRP14 to ribosomal components. (A) Analysis of [^{35}S]-labeled Cyc130 and pPl86 nascent chains of purified RNCs by 5−20% SDS−PAGE. (B) Relative yields of pPl86 and Cyc130 nascent chains at maximized translation efficiencies. The [^{35}S]-labeled polypeptides were quantified with phosphorescence imaging, and their relative yields were calculated taking into account that pPl86 and Cyc130 contain four and six methionine residues, respectively. (C) Immunoblot analysis of the cross-linking reactions with affinity-purified anti-SRP14 antibodies. Complexes formed between SRP (1 pmol) and RNCs (2 pmol) were treated with 800 μM DSS, and the proteins of the different samples were separated by 12% SDS−PAGE. N: ribosomes prepared from mock translations; C: Cyc130 RNCs; P: pPl86 RNCs. Lanes 6−8: RNCs alone and lanes 9−11: RNCs and canine SRP. Control lanes 3−5: RNCs alone without DSS and lanes 1 and 2: canine SRP without and with DSS treatment, respectively. The number following X in the labels indicates the estimated minimal size of the cross-linked ribosomal components. 14-X9 marks the cross-link between SRP14 and SRP9. (D) The relative abundances of the cross-linked products. The cross-linked products in lanes 9−11 were quantified with a CCD camera-based system. The intensities of each cross-linked product were compared to the one in Cyc130 RNC reactions, which was set to 100% (Materials and Methods). (E) Immunoblot analysis of the cross-linking reactions with SRP and wheat germ RNCs using affinity-purified anti-SRP14 antibodies. Cross-linking reactions were done as in panel C. Lanes 1−3: RNCs without DSS; lanes: 4−6: RNCs with DSS; and lanes 7−9: RNCs with SRP and DSS treatment. *: wheat germ ribosomal protein of the small subunit recognized fortuitously by the anti-SRP14 antibodies. MW: molecular weight standards.

and Cyc130 synthesis by titrating the synthetic transcripts into the translation reactions (results not shown, see Materials and Methods). At optimized conditions, the ribosome occupancy with nascent chains in Cyc130 RNC samples was reproducibly 1.6-fold higher as compared to pPl86 RNC samples (Figure 1B). Hence, there were less vacant ribosomes in Cyc130 RNC than in pPl86 RNC samples.

Optimal cross-linking efficiencies with pPl86 RNCs were obtained at a ribosome-SRP ratio of 2:1 as established in experiments described below. Taking into account that SRP binds preferentially to pPl86 RNCs as opposed to vacant ribosomes (*29*), we deduced from this result that the pPl86 RNC preparation contained about 50% vacant ribosomes. On the basis of the higher efficiency of Cyc130 synthesis, the occupancy of ribosomes in Cyc130 RNC preparations could be expected to be around 80%. The optimal DSS concentration in the cross-linking experiments was 800 μM, which is 20-fold higher than the one used in similar experiments that identified ribosomal proteins cross-linked to SRP54 (*18*). The requirement for a higher DSS concentration may be explained by the smaller size and/or lower accessibility of the targets.

With pPl86 RNCs in the cross-linking reaction, the anti-SRP14 antibodies specifically recognized five protein species with higher apparent molecular weights than SRP14 (Figure 1C, lane 11), indicating that they represented SRP14 adducts. With ribosomes from mock translations and with Cyc130 RNCs (Figure 1C, lanes 9 and 10), the antibodies revealed four cross-linked products with the same apparent sizes consistent with the interpretation that the covalent linkages occurred to the same proteins. The cross-link 14-X17 was undetectable. In all cases, the smallest cross-linked species had the expected size of an SRP14-SRP9 adduct. Indeed, it was also seen with SRP alone (Figure 1C, lane 2) and was recognized by anti-SRP9 antibodies (result not shown). The other cross-linked products presumably represented SRP14 covalently linked to ribosomal proteins. The size differences between the apparent molecular weights of the cross-linked products and of SRP14 were in the size range of 17−45 kDa as expected for ribosomal proteins (Figure 1C). Notably, we never observed smaller cross-linked products with different RNC-SRP ratios and with different DSS concentrations, making it unlikely that they represented cross-links between more than two proteins (see also Figure 5).

The fact that SRP14 was cross-linked to ribosomal components in all samples was consistent with the previous observations that SRP could bind directly to ribosomes in a signal sequence- and nascent chain-independent fashion (*25*, *29*−*31*). Moreover, it demonstrated that the *Alu* domain was already in close proximity to the ribosome in the absence of elongation arrest. The 14-X20 product was present at equal intensities in all reactions (Figure 1C), suggesting that it might represent a cross-linked product specific to ribosomes that do not expose a signal sequence. Later experiments showed (see below) that 14-X20 also represented a signal sequence-specific cross-linked product.

Interestingly, upon signal sequence recognition, the other cross-linked products became more abundant. The 14-X45 and 14-X31 signals were reproducibly 2.5-fold higher with pPl86 RNCs than with Cyc130 RNCs (Figure 1C,D and Table 1). Similarly, 14-X17 was only detected with pPl86 RNCs. If this increase was specific for signal sequence

Table 1: Formation and Ribosomal Subunit Association of SRP14 Cross-Linked Products

cross-linked products	with Cyc130 RNC[a]	with pPl86 RNC[a]	in preprolaction translation[b]	in cyclin translation[b]	subunit association
14-X45	+	+++	D	ND	60S
14-X31	+	+++	D	ND	40S
14-X20	+	+	+	++	60S
14-X17	ND	D	D	ND	NA

[a] The intensities of the same cross-linked product formed either with Cyc130 RNCs or with pPl86 RNCs were compared, as presented in Figure 1D. [b] The intensities of the same cross-linked product formed during synthesis of either cyclin or preprolactin were compared, as presented in Figure 2C. The cyclin translation was supplemented with canine SRP. D, detected; ND, not detected; NA, not assigned.

recognition by SRP, it should reach a maximum, once all SRP was bound to ribosomes bearing pPl86 nascent chains (subsequently called pPl86 ribosomes to avoid confusion with pPl86 RNC preparations, which also comprise vacant ribosomes). This hypothesis was tested experimentally by varying the ratio between SRP and number of pPl86 ribosomes in the cross-linking reactions. SRP is expected to bind preferentially to pPl86 ribosomes because of its 2 orders of magnitude higher affinity (*29*). To increase the number of pPl86 ribosomes, we raised the total amount of ribosomes. Specifically, cross-linking reactions with Cyc130 and pPl86 RNCs were done at ribosome−SRP ratios of 2:1 and 3:1. We found that in both cases, 14-X45 and 14-X31 were 2.5-fold more abundant in cross-linking reactions with pPl86 RNCs than with Cyc130 RNCs, confirming that the increase was limited and that the maximum was already reached at the lower ribosome−SRP ratio. To decrease the number of pPl86 ribosomes, we lowered the ribosome occupancy by adding less preprolactin and cyclin mRNAs while keeping the ribosome-SRP ratio at 3:1. At 2.5-fold lower ribosome occupancy as in the previous experiments, 14-X45 and 14-X31 were only 1.6-fold more abundant (results not shown). Presumably, pPl86 ribosomes now become limiting, and SRP was also bound to vacant ribosomes, thereby reducing the increase of 14-X45 and 14-X31. These findings were consistent with the interpretation that the observed changes were specific for pPl86 ribosomes and therefore revealed a noticeable change in the environment of SRP14 upon signal sequence recognition.

As indicated by the strong signal of SRP14 in the control lanes with pPl86 RNCs (Figure 1C, lanes 5 and 8), endogenous rabbit SRP present in the lysate copurified with the RNCs exposing a signal sequence. Hence, the weak signals observed for some adducts in the absence of canine SRP were likely to result from covalent links between rabbit SRP14 and ribosome (Figure 1C, lane 8).

We repeated the cross-linking experiments with wheat germ ribosomes. At maximal translation efficiencies and at a ribosome−SRP ratio of 2:1, we observed cross-linked products of similar sizes (Figure 1E). The 14-X20 adduct was weaker and the 14-X17 adduct stronger than with the mammalian system, which may be explained by structural differences between the systems. However, the proteins, which were in proximity to the *Alu* domain, appeared to be conserved between mammalian and plant ribosomes since both RNC-SRP complexes produced the same number of cross-linked products, and the cross-linked products were of comparable sizes. Note, that even under optimized translation conditions the yield of nascent chains for the same amount of ribosome was significantly lower with wheat germ lysate than with reticulocyte lysate (Materials and Methods). Hence, the observed cross-links might predominantly reflect binding of SRP to vacant ribosomes. It was therefore not surprising that under the experimental conditions used, we failed to observe a difference in the relative intensities of the cross-linked products in the presence of preprolactin nascent chains. In the subsequent experiments, we concentrated our efforts on the characterization of the homologous system.

Cross-Linked Products Reflect Two Functional States of SRP−Ribosome−Nascent Chain Complexes. If the cross-linked species observed with purified RNCs, which were artificially arrested in translation, reflected functional SRP−ribosome complexes, we should be able to detect them in ongoing translation. Reticulocyte lysate translation reactions alone or programmed individually with full-length preprolactin and cyclin synthetic mRNAs were reacted with DSS after 15 min of translation. Both cyclin and preprolactin can be detected at this time point, and the synthetic mRNA concentrations chosen for the cross-linking experiments yielded comparable translation efficiencies for both proteins (Figure 2A,B). After cross-linking, the ribosomes were purified through a high-salt sucrose cushion and analyzed for the presence of SRP14 adducts as before (Figure 2C, upper panel). To confirm that the same amount of ribosomes was analyzed in each sample, we performed immunoblots with anti-S15 antibodies on the same reactions (Figure 2C, lower panel). The lower SRP concentrations in the cyclin and mock translations samples, as reflected by the SRP9-SRP14 signals, were explained by the fact that SRP−ribosome complexes are only stable to high salt treatment in the presence of a signal sequence in the nascent chain (*25*). SRP was therefore removed from ribosome bearing nascent chains lacking a signal sequence and from vacant ribosomes in the high salt purification step, unless it was covalently linked to a ribosomal protein (Figure 2C, lanes 1, 2, 4, and 5).

In one series of translation reactions, cross-linking occurred to the endogenous rabbit SRP (Figure 2C, lanes 1−3). However, since some of the signals were rather weak in these samples, we repeated the same experiments in the presence of additional canine SRP (Figure 2C, lanes 4−6). Cross-linked products of identical sizes as those observed with purified RNCs were unambiguously identified. During preprolactin synthesis, three of the four ribosome-specific adducts were clearly detectable with rabbit SRP alone (Figure 2C, lane 3), whereas based on the abundances of the other adducts, 14-X17 was presumably too faint to be detected. However, it became just detectable after the addition of canine SRP (Figure 2C, lane 6). Hence, rabbit and canine SRP yielded the same adducts during preprolactin synthesis as observed with artificially arrested pPl86 RNCs. This finding confirmed that these cross-linked products defined the environment of SRP14 in functional SRP−ribosome complexes.

During the translation of nascent chains lacking a signal sequence, only 14-X20 was detected (Figure 2C, lane 2). However, it was weaker than in preprolactin translation and was even absent in mock translation (Figure 2C, lane 1).

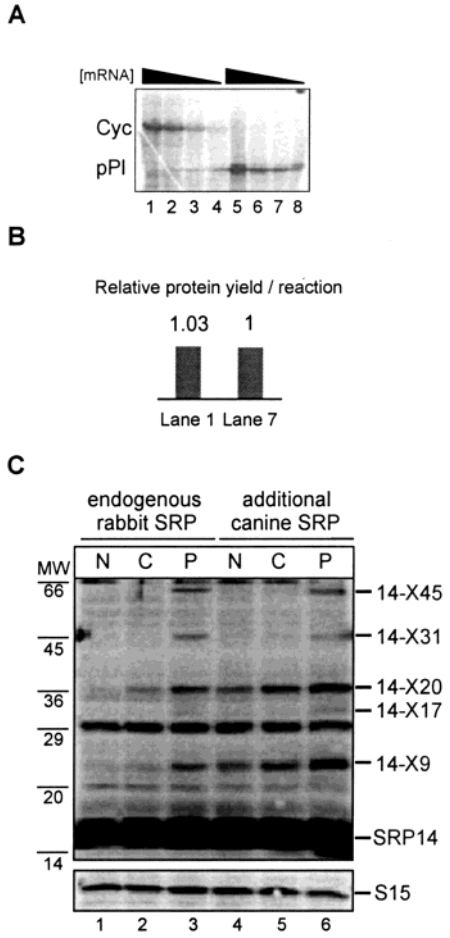

FIGURE 2: Cross-linking of SRP14 to ribosomal components in ongoing translation. (A) Cyclin and preprolactin synthesis analyzed by 5−20% SDS−PAGE and autoradiography. Synthetic cyclin and preprolactin mRNAs were titrated individually into reticulocyte translation reactions in the presence of [^{35}S]-methionine, and the translation products were analyzed after 15 min. (B) Quantification of cyclin and preprolactin by phosphorescence imaging. The relative yields were calculated taking into account that cyclin and preprolactin contain 16 and eight methionine residues, respectively. In lanes 1 and 7, equivalent molar amounts of the full-length proteins were present in the reactions, and these conditions were used for the cross-linking experiments. (C) Immunoblot analysis of the cross-linked products formed between SRP14 and ribosomal components during cyclin and preprolactin synthesis. The ribosomes were purified through high-salt sucrose cushions after cross-linking, and the samples were analyzed by 12% SDS−PAGE (upper panel). N: mock translations; C: cyclin synthesis; and P: preprolactin synthesis. Lanes 4−6 contained additional canine SRP (4 pmol). The same experiment was also analyzed by immunoblotting against anti-S15 antibodies (lower panel). MW: molecular weight standards.

Thus, in contrast to the experiments with artificially arrested RNCs, the abundance of 14-X20 changed markedly in the different samples. Indeed, the changes in the 14-X20 signals appeared to parallel the expected relative affinities of SR for the different ribosomes as characterized for wheat germ ribosomes and canine SRP (*29*). This observation is plausibly rationalized by assuming that other translation factors and/or chaperones may compete with SRP binding to ribosomes (*25*, *32*) in ongoing translation but not in the experiments with artificially arrested, purified RNCs.

In the experiments with artificially arrested RNCs, we observed a signal sequence-specific increase in the relative abundances of several SRP14 adducts. Similarly, the 14-X31 and 14-X45 products were only detected during preprolactin synthesis (Figure 2C, lane 3) in ongoing translation confirming that signal sequence-specific changes occurred at the *Alu* domain−ribosome interface. To exclude the possibility that the 14-X31 and 14-X45 products escaped detection, we increased the cross-linking signals by the addition of canine SRP. Despite the 2-fold increase in 14-X20 during cyclin synthesis (Figure 2C, lane 5) as compared to preprolactin synthesis (Figure 2C, lane 3), 14-X31 and 14-X45 remained undetectable. Hence, unlike with Cyc130 RNCs, their formation was strictly dependent on signal sequence recognition. The presence of small amounts of 14-X45 and 14-X31 in the cross-linking reactions with Cyc130RNCs might be explained by the artificial stabilization of the normally transient interaction of SRP with ribosomes synthesising cytosolic proteins as already discussed.

As mentioned before, SRP does not bind to ribosomes at high salt concentrations (500 mM potassium acetate) in the absence of a signal sequence in the nascent chain. Hence, repeating the cross-linking experiments with pPl86 RNCs at high salt concentrations should allow us to identify the cross-linked products that were specific for the elongation-arrested state of SRP. In these experiments (Figure 3A,B, lanes 3 and 6), we detected four cross-linked products of identical sizes with the same relative abundances at 50 and 500 mM salt. As expected, in the negative controls with Cyc130 RNCs and ribosomes, we failed to detect cross-linked products (Figure 3A, lanes 4 and 5). These results were quite striking and proved that the observed cross-linked products were specific for pPl86 ribosome−SRP complexes. Most importantly, they demonstrated that the interactions between the *Alu* domain and the ribosome were unchanged, suggesting that upon signal sequence recognition the overall position of complete SRP is the same at high salt concentrations.

SRP14 Is Covalently Linked to Proteins of the Small and Large Ribosomal Subunits. To address the question whether SRP14 was cross-linked to bona fide ribosomal proteins that belong to one or both subunits, we dissociated the RNCs after the cross-linking reaction with puromycin and high salt treatments. The subunits were separated by sedimentation through a sucrose gradient. Fractions were collected with continuous monitoring of the absorbance at 254 nm and analyzed by SDS−PAGE followed by immunoblotting with antibodies against SRP14, S15, and L9 (Materials and Methods). Monitoring S15, L9, and the ribosomal RNA allowed us to examine the efficiency of the subunit separation and to identify the fractions comprising the subunits. Without adding DSS to Cyc130 RNCs, all RNCs were separated into subunits (Figure 4A). In contrast, after treatment with DSS at the usual concentration (800 μM), almost all ribosomes were found in the 80S peak, presumably because most of the ribosomal subunits became covalently linked through ribosomal proteins (results not shown). To alleviate this problem, we determined the minimal DSS concentration, which still allowed us to detect the SRP14-adducts (100 μM). Even at the reduced DSS concentration, a significant fraction of the ribosomal subunits were cross-linked (Figure 4B, 80S). As evaluated from the S15 and L9 contents of the 80S fractions, the cross-linked ribosomes represented about 75% (see also Figure 5B,C). Importantly, based on the RNA and

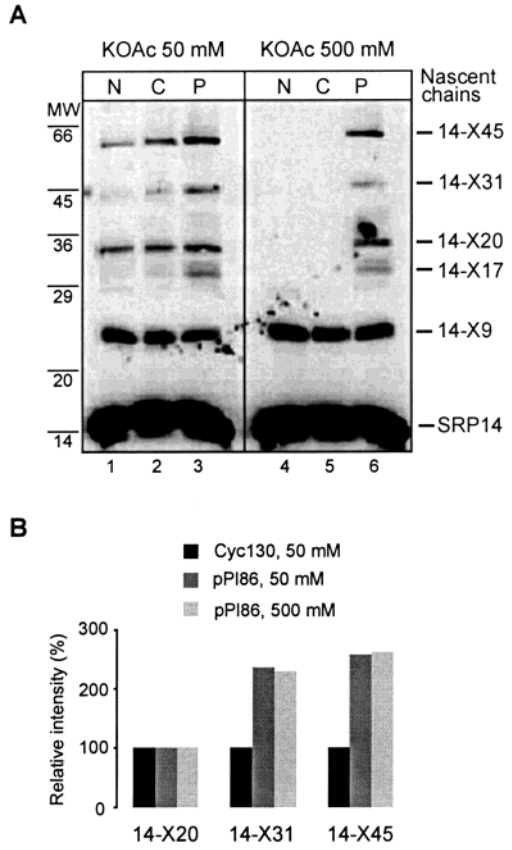

FIGURE 3: Salt-dependent cross-linking of SRP14 to ribosomal components. (A) Immunoblot analysis of the cross-linking reactions with affinity-purified anti-SRP14 antibodies. Complexes formed between SRP (1 pmol) and rabbit RNCs (2 pmol) were treated with 800 μM DSS, and the proteins were displayed by 12% SDS−PAGE. N: ribosomes prepared from mock translations; C: Cyc130 RNCs; and P: pPl86 RNCs. Lanes 1−3 and 4−6: cross-linking reactions at 50 and 500 mM KOAc, respectively. MW: molecular weight standards. (B) Quantification of the cross-linked products in the pPl86 reactions. The cross-linked products in lanes 2, 3, and 6 were quantified with a CCD camera-based system. The intensities of each cross-linked product were compared to the one in Cyc130 RNC reactions at 50 mM salt, which was set to 100% (Materials and Methods).

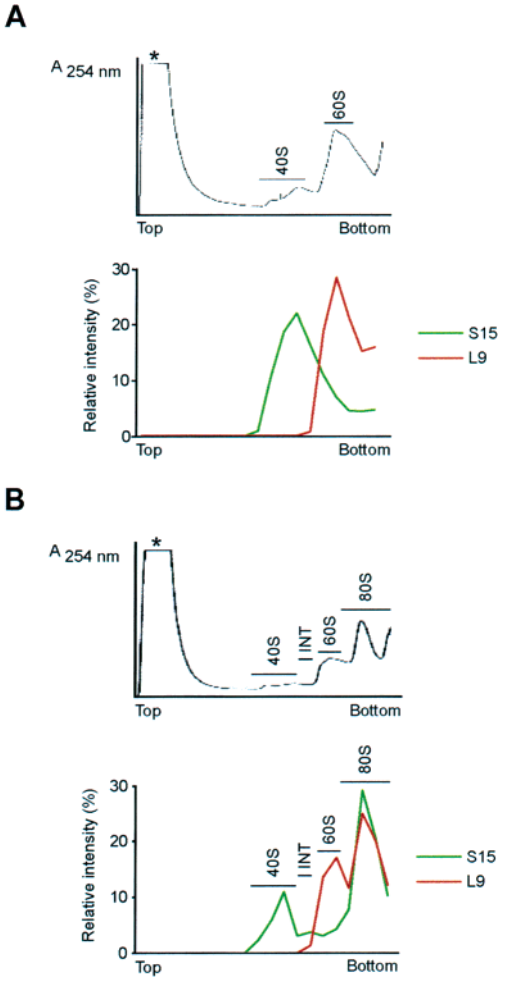

FIGURE 4: Ribosomal subunit separation with and without DSS treatment. (A) RNA, S15, and L9 profiles without DSS treatment. Cyc130 RNCs were treated with puromycin/high salt, and the ribosomal subunits were resolved on a 10−30% sucrose gradient. The absorbance at 254 nm was monitored continuously during fractionation (upper panel). The L9 and S15 contents of all fractions were determined by 12% SDS−PAGE followed by immunoblotting with anti-S15 and anti-L9 antibodies. The signals were quantified with a CCD camera-based system (lower panel). (B) RNA, S15, and L9 profiles with DSS treatment (100 μM). Data were collected as described in panel A. The asterisk denotes free GPT (see Material and Methods).

protein profiles, we could clearly identify the regions in the gradient that comprised the subunits (Figure 4B, upper and lower panel).

To assign the cross-linked products observed with pPl86 RNC-SRP complexes, fractions were collected from a gradient run in parallel. On the basis of the analysis presented in Figure 4, the fractions were pooled to represent the 80S, 60S, and 40S subunits. This was necessary to detect the cross-linked products associated with the subunits with the anti-SRP14 antibodies. The intermediate region (INT) was separated from the subunits because it contained small amounts of L9 and S15 (Figure 4B). The fractions from the top of the gradient were pooled into four equal parts (Figure 5A, fractions 1−4). The S15 and L9 contents of all fractions were determined to verify the assignments (Figure 5A). SRP14 was quantified from a picture taken at a much shorter exposure to monitor the presence of SRP in the different fractions (not shown). About 72% of SRP was not cross-linked to ribosomes and was therefore found on top of the gradient (Figure 5A, lanes 1−3, the presence of SRP was also revealed by the SRP9-SRP14 cross-link). About 16% of the SRP was found in the 80S fractions, whereas only 8 and 4% SRP was present in the 60S and 40S fractions, respectively. Notably, in the experiments with pPl86 RNCs, all four SRP14 adducts were present in the 80S fraction, and none was found at the top of the gradient (Figure 5A,B), confirming unambiguously that SRP14 was cross-linked to bona fide ribosomal proteins.

Of the four cross-linked products, 14-X31 was clearly detected in the 40S fraction (Figure 5A,B and Table 1). In addition, it was more enriched in the 40S fraction as compared to the adjacent fractions further corroborating its association with the small subunit. Note, the 60S fraction was contaminated with the 80S fraction (Figure 4B) and therefore also contained S15 and 14-X31 (Figure 5B). The cross-linked products 14-X20 and 14-X45 were present in the 60S fraction and completely absent in the 40S fraction consistent with the interpretation that both cross-links occurred to the large subunit (Figure 5C,D and Table 1). The weakest cross-linked species, 14-X17, was just detectable in the 60S fraction. However, its abundance was lower as

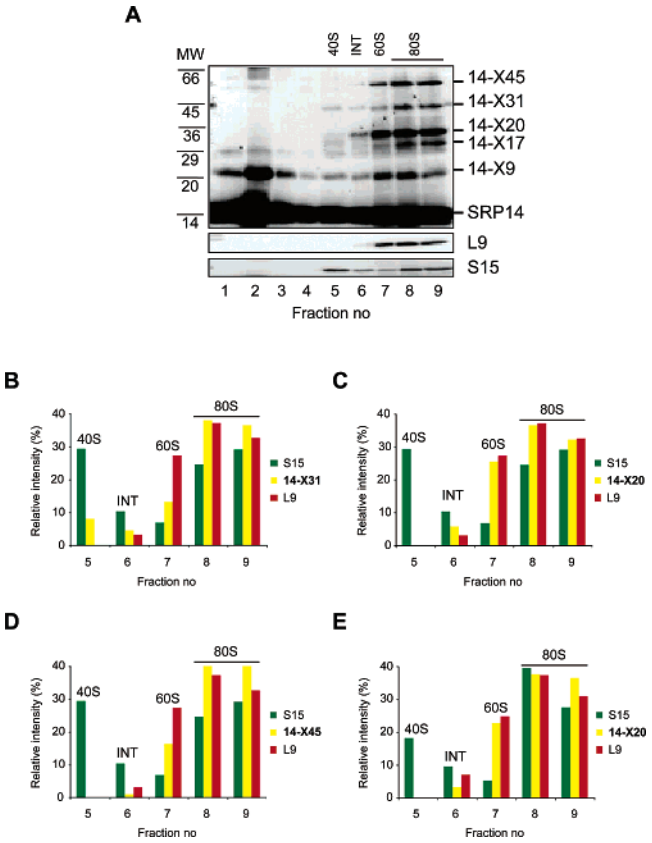

FIGURE 5: Cross-linking of SRP14 to ribosomal subunits. (A) Immunoblot analysis of the gradient after ribosomal subunit separation. pPl86 RNCs (21 pmol) were incubated with canine SRP (17.5 pmol) and treated with DSS (100 μM final concentration) at low salt concentration (50 mM potassium acetate and 2.5 mM Mg(OAc)$_2$). Subsequently, ribosomes were dissociated into subunits by puromycin/high salt treatment, and the subunits were separated on a 10−30% sucrose gradient. Fractions were collected and pooled to represent 40S (lane 5), Int (lane 6), 60S (lane 7), and 80S (lanes 8 and 9) as established in Figure 4. The top fractions were combined into four equal parts (fractions 1−4). All fractions were analyzed by 12% SDS−PAGE and by immunoblotting with anti-SRP14 (upper panel), anti-L9 (medium panel), and anti-S15 (lower panel) antibodies. MW: molecular weight standards. (B−D) Relative amounts of 14-X31 (B), 14-X20 (C), and 14-X45 (D) as compared to the amounts of S15 and L9 present in each fraction. (E) Quantification of a gradient immunoblot analysis of Cyc130 RNCs cross-linked to SRP. Same experimental conditions as in panel A, but the cross-linking reaction was done with Cyc130 RNCs. At DSS concentrations of 100 μM, only 14-X20 could be quantified and was compared to S15 and L9.

compared to 14-X20 and 14-X45, and in the 40S fraction it could not be detected because of a significant background in this region (Figure 5A). Hence, its subunit association could not be determined unambiguously.

We repeated the same experiments with Cyc130 RNCs. At the reduced DSS concentration, the 14-X20, 14-X31, and 14-X45 adducts were detectable in the 80S fraction. However, the latter two were rather weak and therefore almost undetectable in the subunit fractions. We therefore only quantified the 14-X20 adduct. Like with pPl86 RNCs, 14-X20 was completely absent in the 40S fraction but was found in the 60S fraction (Figure 5E) and therefore also represents a covalent link between SRP14 and a protein from the large subunit. Its assignment to the same subunit in experiments with pPl86 and Cyc130 RNCs further supported the interpretation that the 14-X20 cross-linked product was the same in all samples. The fact that SRP14 could be covalently linked to ribosomal proteins of the small and large subunits provides the first experimental evidence that the *Alu* domain of SRP is located in the subunit interface of ribosomes.

DISCUSSION

We have examined the environment of the SRP *Alu* domain bound to ribosomes as a function of signal sequence recognition by SRP in ongoing translation and with artificially arrested RNCs. These studies revealed new mechanistic insights into SRP−ribosome interactions (summarized in Table 1). They provided experimental evidence that the protein SRP14 is in close physical proximity of ribosomal proteins, which could explain the observed delay in nascent chain elongation. In addition, these cross-linked products define binding sites of the SRP *Alu* domain in functional SRP−ribosome complexes comprising conserved ribosomal components as deduced from the comparative analysis of two translation systems. SRP14 cross-linking to ribosomes is independent of signal sequence recognition. However, three of the four cross-linked products become only detectable after signal sequence recognition in ongoing translation. With artificially arrested RNCs, the same cross-linked products were more abundant after signal sequence recognition consistent with a change in the interface of the SRP *Alu* domain and the ribosome. Furthermore, upon signal sequence recognition, the *Alu* domain is located in the ribosomal subunit interface since SRP14 is cross-linked to ribosomal proteins of the small and large subunit. Taken together, these findings indicate that the SRP *Alu* domain can bind to ribosomes in the absence of a signal sequence and changes its environment after signal sequence recognition.

The fact that SRP14 could be cross-linked to ribosomes synthesizing a cytoplasmic protein in a functional translation system confirmed the notion that SRP binds transiently to all actively translating ribosomes (*33*). Furthermore, it demonstrated that the *Alu* domain is already in close contact with the ribosome without signal sequence recognition by SRP. Signal sequence-independent binding of SRP to ribosomes is thought to facilitate the identification of ribosome-nascent chain complexes that need to be targeted to the ER. It has previously been noticed that SRP subunits lacking the *Alu* domain or *Alu* domain components have a strongly reduced capacity to bind ribosomes directly in a signal sequence-independent way (*25, 31*). On the basis of these previous observations, our finding that the *Alu* domain is already in contact with the ribosome in the absence of a signal sequence argues in favor of an active role of the *Alu* domain in direct ribosome binding of SRP. Without a signal sequence, SRP14 is predominantly cross-linked to the large ribosomal subunit. The cross-linked product 14-X20 therefore defines binding of SRP to actively translating ribosomes in the absence of a signal sequence.

Upon signal recognition, the *Alu* domain of SRP delays elongation of the nascent chain and is therefore expected to be located in a position in which it can interfere with the ribosomal elongation cycle. This could be achieved by preventing the entry and the exit of tRNAs at the E- and A-sites, respectively. The four cross-linked products observed at this stage reflect this position since they are specific for

pPl86 ribosomes as indicated by their presence at high salt concentrations, by their formation during preprolactin synthesis, and by the results of the titration experiments with artificially arrested RNCs. This position is undoubtedly located at the subunit interface of the ribosome as proven by the association of the cross-linked products with both ribosomal subunits. To be linked covalently to ribosomal proteins of both subunits, SRP14 would have to span the intersubunit space. On the basis of the crystal structure of the SA50 *Alu* RNP (*24*), the two most distant, solvent-accessible lysine residues (K74 and K95) are separated by about 47 Å. Adding twice the size of the cross-linker increases the maximal distance between two proteins cross-linked to SRP14 to about 74 Å, which is sufficient to bridge the intersubunit space, with each extremity of SRP14 pointing toward one of the ribosomal subunits. Moreover, to position the *Alu* domain at the subunit interface, SRP has to span the distance between the interface and the nascent chain exit site, where SRP54 is located in proximity to L23a and L35 (*18*). According to its size (23−24 nm), SRP is sufficiently extended to contact the two positions simultaneously as previously described (*34*).

Elongation arrest is strictly dependent on the presence of a signal sequence at the nascent chain exit site. Our observations reveal that, upon signal sequence recognition, the interface between the *Alu* domain and the ribosome changes. Hence, a signal has to be sent out from the SRP S domain close to the nascent chain exit site, triggering conformational changes at the *Alu* domain−ribosome interface. The SRP RNA might be involved, as it supports multiple conformations during the SRP cycle (*35*). The signal might act directly on the conformation of the *Alu* domain, which has been suggested to exist in two conformations (*36*). Alternatively, or in addition, flexible domains of the ribosome might be rearranged by long-range interactions within the ribosomal structure (*37*, *38*). Once in the elongation-arrested state, the SRP *Alu* domain is likely to make additional contacts with the ribosome. The changes in the environment of SRP14 and the gain of high salt-resistant cross-linking of SRP14 to ribosomes argue in favor of additional contacts between the *Alu* domain and the ribosome. The components in SRP that mediate these additional contacts remain to be determined. The C-terminal region of SRP14, which is essential for elongation arrest activity (*12*), may contribute to mediating these contacts.

As judged by the sizes of the two largest cross-linked products, the *Alu* domain may be located in proximity to the ribosomal A-site. Since the apparent molecular size of a cross-linked product defines the minimal size of the cross-linked protein, only two proteins, L3 and L4, of all mammalian ribosomal proteins may account for the X45 protein having a size larger than 36 kDa (ref *39*, for a compilation of all ribosomal protein sequences, see the Swiss-Prot Protein Knowledgebase). Alternatively, 14-X45 may represent a cross-link between SRP14 and two ribosomal proteins. We cannot completely exclude this possibility, but it seems rather unlikely for at least two reasons. Since the cross-linking efficiency is very low in our experiments, simultaneous linkage of three proteins is statistically a very rare event, and the 14-X45 cross-linked product would therefore be expected to be much less abundant. In addition, we never observed different cross-linked products of smaller

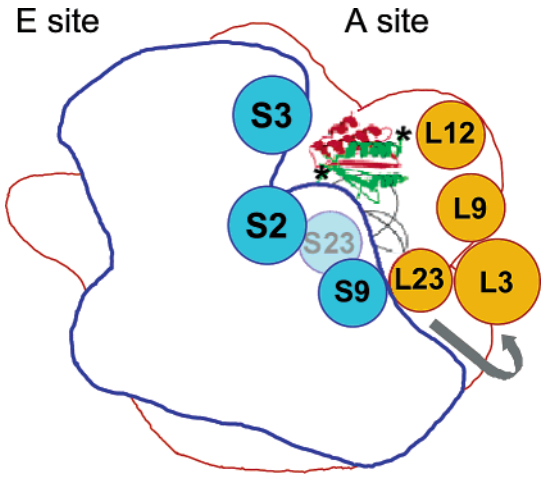

FIGURE 6: Schematic representation of a model for the SRP *Alu* domain location within ribosomes. Complete ribosomes are represented schematically as viewed from the solvent side of the 40S subunit. Ribosomal proteins are positioned in agreement with the cryo-EM reconstructions of yeast ribosomes (*42*). The *Alu* domain is represented at scale by the SA50 *Alu* RNP structure (*36*). Its orientation was chosen randomly. The asterisk represents the two lysine residues at the most distant locations. Gray arrow indicates a possible pathway for the SRP RNA stem linking the *Alu* and S domain.

sizes by changing the experimental conditions (e.g., DSS concentration, salt concentration, RNC-SRP ratio). On the basis of structural and biochemical studies on archaeal and eukaryotic ribosomes (*40*−*43*), only L3 is located at the subunit interface, designating it as a strong candidate for the X45 protein since it may account for both the size of the cross-linked product as well as the location of the *Alu* domain at the subunit interface of ribosomes. Hence, cross-links between SRP14 and L3 place the *Alu* domain in the subunit interface close to the A-site (Figure 6). On the basis of their sizes and on their location with respect to L3, plausible candidates for the other cross-linked ribosomal proteins are L23, L12, and L9 in the large subunit as well as S2, S3, S9, and S23 in the small subunit. S2 and S3 may account for the size of the X31 protein. Although portions of S2 and S3 are exposed at the outer surface of the ribosome, both proteins also reach into the interface, as they can be cross-linked to 28S rRNA (*43*), and S2 is also cross-linked to P0 (a stalk protein) in the large subunit (*44*). Hence, they are strong candidates for the X31 protein. The other possible candidates, L23, L12, L9, S9, and S23, have molecular sizes in the range of 15−22 kDa and are therefore plausible candidates for the X20 and X17 proteins.

Multiple attempts to identify the cross-linked ribosomal proteins using antibodies against several putative candidates for the cross-linked proteins failed to yield irrefutable evidence for their identity. This may be explained by the accumulation of several aggravating factors, including the lack of sensitivity and specificity of the antibodies against ribosomal proteins. We are therefore convinced that the unambiguous identification will require the use of in vitro reconstituted SRP including a labeled or tagged SRP14 protein. However, we have not yet succeeded in obtaining ribosomal cross-links by using SRP reconstituted in vitro from recombinant proteins. In addition, cross-linking experiments with SRP9/14 protein alone and with purified *Alu* RNPs gave apparently different cross-linked products than

did authentic SRP (L. Terzi, and K. Strub, unpublished results). Hence, the cross-linked products could not be identified using labeled SRP9/14 protein alone or purified *Alu* RNPs. Such an approach has been successfully used to identify the ribosomal proteins covalently linked to SRP54 (*18*).

Our studies provide experimental evidence for a long-standing notion that the *Alu* domain may bind at the ribosomal interface, possibly in proximity to the ribosomal A-site. In the future, they will guide us in finding its binding partners in the ribosome to understand the mechanistic implications of the interactions between the SRP *Alu* domain and the ribosomes.

REFERENCES

1. Keenan, R. J., Freymann, D. M., Stroud, R. M., and Walter, P. (2001) The Signal Recognition Particle, *Annu. Rev. Biochem. 70*, 755−775.
2. Walter, P., and Blobel, G. (1981) Transloction of proteins across the endoplasmic reticulum. III. Signal recognition protein (SRP) causes signal sequence and site specific arrest of chain elongation that is released by microsomal membranes, *J. Cell. Biol. 91*, 557−561.
3. Lipp, J., Dobberstein, B., and Haeuptle, M.-T. (1987) Signal Recognition Particle Arrest Elongation of Nascent Secretory and Membrane Proteins at Multiple Sites in a Transient Manner, *J. Biol. Chem. 262*, 1680−1684.
4. Gilmore, R., Walter, P., and Blobel, G. (1982) Protein Translocation Across the Endoplasmic Reticulum. II. Isolation and characterization of the Signal Recognition Particle Receptor, *J. Cell Biol. 95*, 470−477.
5. Meyer, D. I., Krause, E., and Dobberstein, B. (1982) Secretory protein translocation across membranes−the role of the docking protein, *Nature 297*, 647−650.
6. Rapoport, T. A., Rolls, M. M., and Jungnickel, B. (1996) Approaching the mechanism of protein transport across the ER membrane, *Curr. Opin. Cell Biol. 8*, 499−504.
7. Johnson, A. E., and van Waes, M. A. (1999) The translocon: a dynamic gateway at the ER membrane, *Annu. Rev. Cell. Dev. Biol. 15*, 799−842.
8. Miller, J. D., Tajima, S., Lauffer, L., and Walter, P. (1995) The β subunit of the signal recognition particle receptor is a transmembrane GTPase that anchors the α subunit, a peripheral membrane GTPase, to the endoplasmic reticulum membrane, *J. Cell Biol. 128*, 273−282.
9. Connolly, T., and Gilmore, R. (1989) The signal recognition particle receptor mediates the GTP-dependent displacement of SRP from the signal sequence of the nascent polypeptide, *Cell 57*, 599−610.
10. Siegel, V., and Walter, P. (1988) Each of the Activities of Signal Recognition Particle (SRP) Is Contained within a Distinct Domain: Analysis of Biochemical Mutants of SRP, *Cell 52*, 39−49.
11. Wolin, S. L., and Walter, P. (1989) Signal recognition particle mediates a transient elongation arrest of preprolactin in reticulocyte lysate, *J. Cell Biol. 109*, 2617−2622.
12. Thomas, Y., Bui, N., and Strub, K. (1997) A truncation in the 14 kDa protein of the signal recognition particle leads to tertiary structure changes in the RNA and abolishes the elongation arrest activity of the particle, *Nucleic Acids Res. 25*, 1920−1929.
13. Mason, N., Ciufo, L. F., and Brown, J. D. (2000) Elongation arrest is a physiologically important function of signal recognition particle, *EMBO J. 19*, 4164−4174.
14. Siegel, V., and Walter, P. (1986) Removal of the Alu structural domain from signal recognition particle leaves its protein translocation activity intact, *Nature 320*, 81−84.
15. Wiedmann, M., Kurzchalia, T. V., Bielka, H., and Rapoport, T. A. (1987) Direct probing of the interaction between the signal sequence of nascent preprolactin and the signal recognition particle by specific cross-linking, *J. Cell Biol. 104*, 201−208.
16. Garcia, P. D., and Walter, P. (1988) Full-length prepro-α-factor can be translocated across the mammalian microsomal membrane only if translation has not terminated, *J. Cell Biol. 106*, 1043−1048.
17. Bacher, G., Lütcke, H., Jungnickel, B., Rapoport, T. A., and Dobberstein, B. (1996) Regulation by the ribosome of the GTPase of the signal-recognition particle during protein targeting (see comments), *Nature 381*, 248−251.
18. Pool, M. R., Stumm, J., Fulga, T. A., Sinning, I., and Dobberstein, B. (2002) Distinct modes of signal recognition particle interaction with the ribosome, *Science 297*, 1345−1348.
19. Beckmann, R., Spahn, C. M., Eswar, N., Helmers, J., Penczek, P. A., Sali, A., Frank, J., and Blobel, G. (2001) Architecture of the protein-conducting channel associated with the translating 80S ribosome, *Cell 107*, 361−372.
20. Gu, S. Q., Peske, F., Wieden, H. J., Rodnina, M. V., and Wintermeyer, W. (2003) The signal recognition particle binds to protein L23 at the peptide exit of the *Escherichia coli* ribosome, *RNA 9*, 566−573.
21. Rinke-Appel, J., Osswald, M., von Knoblauch, K., Mueller, F., Brimacombe, R., Sergiev, P., Avdeeva, O., Bogdanov, A., and Dontsova, O. (2002) Cross-linking of 4.5S RNA to the *Escherichia coli* ribosome in the presence or absence of the protein Ffh, *RNA 8*, 612−625.
22. Zwieb, C. (1985) The secondary structure of the 7SL RNA in the signal recognition particle: functional implications, *Nucleic Acids Res. 13*, 6105−6124.
23. Walter, P., and Lingappa, V. R. (1986) Mechanism of Protein Translocation Across the Endoplasmic Reticulum Membrane, *Annu. Rev. Cell Biol. 2*, 499−516.
24. Weichenrieder, O., Wild, K., Strub, K., and Cusack, S. (2000) Structure and assembly of the Alu domain of the mammalian signal recognition particle, *Nature 408*, 167−173.
25. Powers, T., and Walter, P. (1996) The nascent polypeptide-associated complex modulates interactions between the signal recognition particle and the ribosome, *Curr. Biol. 6*, 331−338.
26. Neuhof, A., Rolls, M. M., Jungnickel, B., Kalies, K. U., and Rapoport, T. A. (1998) Binding of signal recognition particle gives ribosome/nascent chain complexes a competitive advantage in endoplasmic reticulum membrane interaction, *Mol. Biol. Cell 9*, 103−115.
27. Bovia, F., Fornallaz, M., Leffers, H., and Strub, K. (1995) The SRP9/14 subunit of the signal recognition particle (SRP) is present in more than 20-fold excess over SRP in primate cells and exists primarily free but also in complex with small cytoplasmic Alu RNAs, *Mol. Biol. Cell 6*, 471−484.
28. Walter, P., and Blobel, G. (1983) Signal recognition particle: a ribonucleoprotein required for cotranslational translocation of proteins, isolation, and properties, *Methods Enzymol. 96*, 682−691.
29. Flanagan, J. J., Chen, J. C., Miao, Y., Shao, Y., Lin, J., Bock, P. E., and Johnson, A. E. (2003) Signal recognition particle binds to ribosome-bound signal sequences with fluorescence-detected subnanomolar affinity that does not diminish as the nascent chain lengthens, *J. Biol. Chem. 278*, 18628−18637.
30. Walter, P., Ibrahimi, I., and Blobel G. (1981) Translocation of Proteins across the Endoplasmic Reticulum I. Signal Recognition Protein (SRP) Binds to in Vitro Assembled Polysomes Synthesizing Secretory Protein, *J. Cell Biol. 91*, 545−550.
31. Hauser, S., Bacher, G., Dobberstein, B., and Lutcke, H. (1995) A complex of the signal sequence binding protein and the SRP RNA promotes translocation of nascent proteins, *EMBO J. 14*, 5485−5493.
32. Thulasiraman, V., Yang, C. F., and Frydman, J. (1999) In vivo newly translated polypeptides are sequestered in a protected folding environment, *EMBO J. 18*, 85−95.
33. Ogg, S. C., and Walter, P. (1995) SRP samples nascent chains for the presence of signal sequences by interacting with ribosomes at a discrete step during translation elongation, *Cell 81*, 1075−1084.
34. Andrews, D. W., Walter, P., and Ottensmeyer, F. P. (1985) Structure of the signal recognition particle by electron microscopy, *Proc. Natl. Acad. Sci. U.S.A. 82*, 785−789.
35. Andreazzoli, M., and Gerbi, S. A. (1991) Changes in 7SL RNA conformation during the signal recognition particle cycle, *EMBO J. 10*, 767−777.

36. Weichenrieder, O., Stehlin, C., Kapp, U., Birse, D. E., Timmins, P. A., Strub, K., and Cusack, S. (2001) Hierarchical assembly of the Alu domain of the mammalian signal recognition particle, *RNA 7*, 731−740.
37. Agrawal, R. K., Heagle, A. B., Penczek, P., Grassucci, R. A., and Frank, J. (1999) EF-G-dependent GTP hydrolysis induces translocation accompanied by large conformational changes in the 70S ribosome, *Nat. Struct. Biol. 6*, 643−647.
38. Gomez-Lorenzo, M. G., Spahn, C. M., Agrawal, R. K., Grassucci, R. A., Penczek, P., Chakraburtty, K., Ballesta, J. P., Lavandera, J. L., Garcia-Bustos, J. F., and Frank, J. (2000) Three-dimensional cryo-electron microscopy localization of EF2 in the *Saccharomyces cerevisiae* 80S ribosome at 17.5 Å resolution, *EMBO J. 19*, 2710−2718.
39. Wool, I. G., Chan, Y. L., and Gluck, A. (1995) Structure and evolution of mammalian ribosomal proteins, *Biochem. Cell Biol. 73*, 933−947.
40. Ban, N., Nissen, P., Hansen, J., Moore, P. B., and Steitz, T. A. (2000) The complete atomic structure of the large ribosomal subunit at 2.4 Å resolution, *Science 289*, 905−920.
41. Yusupov, M. M., Yusupova, G. Z., Baucom, A., Lieberman, K., Earnest, T. N., Cate, J. H., and Noller, H. F. (2001) Crystal structure of the ribosome at 5.5 Å resolution, *Science 292*, 883−896.
42. Spahn, C. M., Beckmann, R., Eswar, N., Penczek, P. A., Sali, A., Blobel, G., and Frank, J. (2001) Structure of the 80S ribosome from *Saccharomyces cerevisiae*—tRNA−ribosome and subunit−subunit interactions, *Cell 107*, 373−386.
43. Nygard, O., and Nika, H. (1982) Identification by RNA-protein cross-linking of ribosomal proteins located at the interface between the small and the large subunits of mammalian ribosomes, *EMBO J. 1*, 357−362.
44. Uchiumi, T., Kikuchi, M., and Ogata, K. (1986) Cross-linking study on protein neighborhoods at the subunit interface of rat liver ribosomes with 2-iminothiolane, *J. Biol. Chem. 261*, 9663−9667.

BI0353777